Research Square

Preprints are preliminary reports that have not undergone peer review.
They should not be considered conclusive, used to inform clinical practice,
or referenced by the media as validated information.

Membrane pre-concentration ahead of MEA absorption: a rate-based, mixed-gas techno-economic assessment for natural gas, coal and cement flue gases

Miracle Ajoku

miracleajoku96@gmail.com

Federal University of Technology Owerri https://orcid.org/0009-0001-2256-3651

Research Article

Keywords: post-combustion CO2 capture, hybrid membrane–amine process, monoethanolamine, rate-based modelling, dual-mode sorption, Matrimid 5218, techno-economic analysis

Posted Date: November 10th, 2026

DOI: https://doi.org/10.21203/rs.3.rs-11674132/v1

License: This work is licensed under a Creative Commons Attribution 4.0 International License.
Read Full License

Additional Declarations: The authors declare no competing interests.

Membrane pre-concentration ahead of MEA absorption: a rate-based, mixed-gas techno-economic assessment for natural gas, coal and cement flue gases

Miracle Victory Ajoku*

Department of Chemical Engineering, Federal University of Technology Owerri, Nigeria
*Corresponding author. E-mail: miracleajoku96@gmail.com

Abstract

Membrane pre-concentration of flue gas ahead of an amine absorber is frequently proposed as a route to lower the energy and size of post-combustion CO_2 capture. Two questions are rarely examined together: how much an MEA plant actually gains from a CO_2-enriched feed, and whether membrane stages sized with pure-gas permeability data deliver the separation assumed in such hybrid designs. This work addresses both using a rate-based MEA model and a competitive dual-mode hollow-fibre membrane model. The MEA model (ENRTL-RK thermodynamics, rate-based packed columns) was validated against the Kaiserslautern pilot plant, reproducing CO_2 removal within 0.1 percentage points of the AspenTech reference model and within 3.6 points of measurement, and was then scaled to an industrial plant on the NETL natural gas combined cycle (NGCC) baseline. At the optimal lean loading of 0.20, the reference plant requires a specific reboiler duty (SRD) of 3.88 GJ t^{-1} CO_2. An amine performance map spanning 4.5 to 40 vol% CO_2 (dry) shows that SRD falls only to 3.58 GJ t^{-1} and is nearly flat above 20 to 30 vol%, because rich loading approaches its ceiling while the hotter rich solvent pinches the lean/rich exchanger. Coupling this map with a Matrimid 5218 membrane stage designed to pass 94.7% of the CO_2 to the absorber, hybrid configurations for NGCC (4.5% CO_2), coal (14.7%) and cement (20%) flue gases consumed 41 to 280% more equivalent energy and cost USD 22 to 1057 t^{-1} CO_2 more than MEA alone. The hybrid remained more expensive under every combination of assumptions tested, including a membrane of zero cost, and a high-performance membrane (1000 GPU, CO_2/N_2 selectivity of 50) reduced but did not remove the penalty (USD 7 to 80 t^{-1} CO_2 at base assumptions, and at least USD 7 t^{-1} with a free membrane). Designing the membrane with pure-gas data undersized compression-driven stages by up to 6.5% and reduced overall capture from 90% to as low as 88.7%, whereas vacuum-driven stages were unaffected. The results indicate that single-stage membrane pre-concentration is not justified ahead of 30 wt% MEA for these sources, and that mixed-gas transport must be accounted for wherever glassy-polymer membrane feeds are compressed.

Keywords: post-combustion CO_2 capture; hybrid membrane–amine process; monoethanolamine; rate-based modelling; dual-mode sorption; Matrimid 5218; techno-economic analysis

Highlights

- Rate-based MEA model validated against pilot data and scaled to the NETL NGCC baseline.
- Specific reboiler duty falls only from 3.88 to 3.58 GJ t^{-1} as feed CO_2 rises from 4.5 to 40%.
- Membrane pre-concentration raises cost by USD 22 to 1057 t^{-1} CO_2 for NGCC, coal and cement.
- The hybrid remains uneconomic in every sensitivity case, including a free membrane and a 1000 GPU, selectivity-50 membrane.
- Pure-gas design undersizes compression-driven membranes by up to 6.5%; vacuum designs are unaffected.

Nomenclature

Symbol	Description (units)
a	Membrane area per unit module length (m^2 m^{-1})
b_i	Langmuir affinity constant of gas i (bar^{-1})
$C_{D,i}$, $C_{H,i}$	Henry and Langmuir sorbed concentrations (cm^3(STP) cm^{-3})
$C'_{H,i}$	Langmuir capacity (cm^3(STP) cm^{-3})
$D_{D,i}$, $D_{H,i}$	Diffusivities of Henry and Langmuir populations (cm^2 s^{-1})
F, K	Mobility ratio D_H/D_D and Langmuir-to-Henry capacity ratio (–)
$k_{D,i}$	Henry sorption coefficient (cm^3(STP) cm^{-3} bar^{-1})
P_i	Permeability (Barrer)
p_f, p_p	Feed and permeate pressure (bar)
Q_{reb}	Reboiler duty (MW)
R_{mem}	Membrane CO_2 recovery to permeate (–)
SRD	Specific reboiler duty (GJ t^{-1} CO_2)
TAC	Total annualised cost of compared items (USD y^{-1})
θ	Steam-to-power equivalence factor (MW_e MW_{th}^{-1})
φ	Dimensionless module flow parameter (–)
η	Isentropic efficiency (–)

1. Introduction

Chemical absorption with aqueous monoethanolamine (MEA) remains the reference technology for post-combustion CO_2 capture, owing to its maturity and its ability to treat large volumes of dilute, near-atmospheric flue gas [1]. Its principal drawback is the thermal energy required to regenerate the solvent, typically 3.5 to 4.0 GJ per tonne of CO_2 for 30 wt% MEA [2], together with the large absorber volumes needed when the CO_2 partial pressure is low.

Membrane separation offers a complementary set of properties: no regeneration heat, modular construction and good performance at high CO_2 concentration, but a strong dependence on pressure ratio and selectivity that makes high recovery from dilute flue gas expensive [3], [4]. Pilot and techno-economic work on post-combustion membranes has identified compression equipment as the dominant cost and favoured permeate vacuum over feed compression [3], [5].

These complementary characteristics have motivated hybrid processes that combine membranes with chemical absorption. Membrane Technology and Research (MTR) and the University of Texas at Austin evaluated membrane–absorption hybrids for coal-fired power plants at bench and pilot scale, combining a membrane contactor with a 5 m piperazine absorber and advanced flash stripper in series and parallel arrangements; they found the parallel arrangement superior but concluded that the hybrid did not achieve a materially lower cost of capture than the piperazine process alone [6]. Cormos et al. assessed several MDEA-based solvent–membrane configurations for supercritical coal plants, including a membrane placed ahead of the absorber with feed compression or permeate vacuum, and found that chemical absorption alone retained a higher net efficiency than the hybrids examined [7]. Membrane pre-concentration has also been combined with CO_2 liquefaction, with an optimum permeate of 65 to 67% CO_2 and a cost of CO_2 avoided about 9% below MEA at 85% capture [8]. Conclusions therefore depend strongly on the solvent, the membrane performance, the process arrangement and the capture target. In the configuration examined here, a membrane stage enriches the flue gas before it reaches an amine absorber. The underlying argument is intuitive: a CO_2-rich feed raises the driving force in the absorber, increases rich loading, shrinks the column and lowers the solvent circulation and regeneration duty. Whether those benefits outweigh the energy and capital of the membrane stage depends on two quantities that are often treated loosely. The first is the response of a real MEA plant to feed enrichment: if SRD decreases only marginally as the CO_2 fraction increases, the thermal saving available to offset membrane compression is small. The second is the accuracy of the membrane design itself. The flattening of amine regeneration energy at high CO_2 partial pressure is known qualitatively; what is lacking is its quantification with a pilot-validated, rate-based model over the composition range relevant to pre-concentration, together with the mechanism that limits it.

Glassy polymers such as Matrimid 5218 transport CO_2 through a dual-mode mechanism in which Henry-type dissolution coexists with sorption in non-equilibrium Langmuir sites [9]. In gas mixtures, CO_2 and N_2 compete for the same Langmuir sites, so that the permeability of each gas depends on the partial pressures of both [10]. Process designs nevertheless commonly

rely on pure-gas permeabilities measured at a single reference pressure. A preceding study [11] showed for Matrimid 5218 hollow fibres that such pure-gas designs overestimate CO_2 recovery by 2.5 to 3.5 percentage points and undersize modules by 5.6 to 9.6% under representative conditions, and that below a CO_2 feed partial pressure of about 0.84 bar the error cannot be removed by re-referencing the pure-gas data at stage cuts of about 10 to 13%, a regime that contracts as the stage cut increases. The same study placed NGCC flue gas compressed to 10 bar in this uncorrectable regime and cement-kiln feeds in a regime correctable by routine testing. That analysis was confined to the module level; its consequences for a complete capture plant were not examined.

This work extends the analysis to the process scale and asks whether membrane pre-concentration ahead of MEA is justified, and whether the pure-gas design error alters that judgement. Compared with earlier hybrid studies [6]–[8], it couples a pilot-validated rate-based amine model with a competitive mixed-gas membrane model, evaluates three flue gas sources on a common basis, and bounds the economic outcome with a zero-cost membrane and a high-performance membrane. Its distinctive contribution is the quantification, at plant scale, of the error introduced by designing glassy-polymer membrane stages with pure-gas data. The specific contributions are: (i) a rate-based MEA model validated against pilot-plant data and scaled to an industrial plant on the U.S. National Energy Technology Laboratory (NETL) NGCC baseline [12]; (ii) an amine performance map quantifying SRD, solvent circulation and absorber size from 4.5 to 40 vol% CO_2, together with the mechanism that limits the benefit of enrichment; (iii) an integrated energy and cost comparison of MEA-only and hybrid plants for NGCC, supercritical pulverised coal [12] and cement [13] flue gases; (iv) a quantification of the error introduced by designing the membrane with pure-gas rather than mixed-gas transport data, across the plausible range of the dual-mode mobility parameter; (v) a sensitivity analysis testing whether any combination of economic and technical assumptions reverses the conclusion; and (vi) a bounding case with a high-performance, Polaris-type membrane to test whether the conclusion depends on the choice of Matrimid.

2. Methodology

2.1 Process configurations and study design

Two configurations were compared for each flue gas source (Fig. 1). In the MEA-only reference, the flue gas is cooled in a direct-contact cooler (DCC), pressurised by a blower and treated in a 30 wt% MEA absorber–stripper plant that captures 90% of the CO_2, which is then

compressed to 15.3 MPa. In the hybrid, a Matrimid hollow-fibre membrane stage driven by feed compression, permeate vacuum or both transfers a fraction R_{mem} of the CO_2 to the permeate, which is fed to the MEA plant; the retentate is vented. With the amine plant capturing 95% of the CO_2 it receives, overall capture of 90% requires $R_{mem} = 0.90/0.95 = 0.947$. All cases were compared at the same CO_2 flow (1411.7 kmol h^{-1}, corresponding to one of four parallel trains of the NETL NGCC plant), so that only the accompanying inert gas differed between sources. CO_2 compression was evaluated for the reference plant; because the CO_2 product is the same in all cases, it cancels in the comparison.

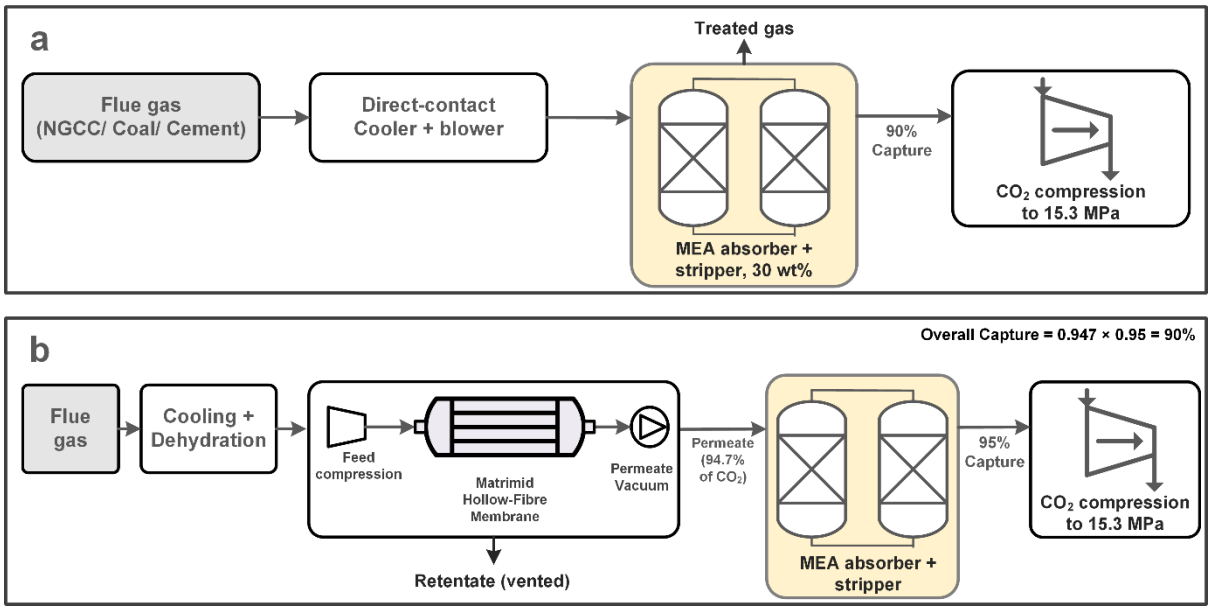


Fig. 1. Process configurations compared in this work. (a) MEA-only reference plant. (b) Hybrid plant in which a Matrimid hollow-fibre membrane stage, driven by feed compression and/or permeate vacuum, transfers 94.7% of the CO_2 to the MEA plant; with 95% capture in the amine plant, overall capture is 90%.

2.2 Rate-based MEA model

The MEA plant was modelled in Aspen Plus V14 using the true-species electrolyte framework of the AspenTech rate-based MEA model [14]. Liquid-phase non-ideality is described by the unsymmetric electrolyte NRTL model and the vapour phase by the PC-SAFT equation of state (ENRTL-RK property method), with parameters regressed by Zhang et al. [15]. The solution chemistry comprises water ionisation, the first and second dissociation of dissolved CO_2, protonation of MEA and carbamate hydrolysis. The reactions of CO_2 with MEA and with OH^- are rate-controlled, with forward kinetics from Hikita et al. [16] and Pinsent et al. [17] and reverse rates obtained from the equilibrium constants. Both columns were modelled with the RateSep rate-based formulation, using the Bravo et al. correlations for mass transfer coefficients and interfacial area [18], the Chilton–Colburn analogy for heat transfer, the Stichlmair et al. correlation for liquid holdup in the stripper [19], a discretised liquid film (five

points, geometric spacing) and a vapour-plug flow model. Argon, present in the industrial flue gases, was added to the component set; its dielectric constant was taken equal to that of water, an assumption without measurable effect given its sub-1% concentration and absence from the reactive liquid.

The model was validated against case 1 of the Kaiserslautern pilot plant [20], which treats a synthetic flue gas of 8.5 wt% CO_2 with 27.5 wt% MEA in a 0.125 m diameter absorber (4.2 m packing plus 0.42 m water wash) and stripper (2.5 m plus 0.42 m), both packed with Mellapak 250.Y (represented by FLEXIPAC 250Y in the AspenTech model). All feed conditions, column geometries and operating specifications were taken from the reported case, and the flowsheet was closed with water and MEA make-up balances.

2.3 Industrial reference plant

The industrial reference plant was designed for one of four parallel trains of NETL Case B31B.90, an F-class NGCC plant with 90% capture and 645 MW_e net output [12]. The design basis is summarised in Table 1. The flue gas leaving the heat recovery steam generator (99 °C, 0.10 MPa) is pressurised to 1.05 bar by a blower (isentropic efficiency 0.85) and cooled to 40 °C in the DCC, which condenses excess water. The 30 wt% MEA solvent (CO_2-free basis) enters the absorber at 40 °C. The absorber contains 20 m of FLEXIPAC 250Y in two beds and the stripper 15 m in two beds; both were discretised into segments of 0.4 m and 0.5 m respectively, and their diameters were fixed to give approximately 70% of flooding capacity in the most loaded bed. The stripper operates at 2.0 bar with a partial condenser at 40 °C and a kettle reboiler. A lean/rich heat exchanger with a minimum approach temperature of 10 K anywhere in the exchanger recovers heat from the lean solvent, which is then trimmed to 40 °C. The treated gas is cooled to 40 °C to recover water and entrained MEA, which are returned to the solvent loop. Capture was held at 90% by adjusting the solvent circulation, and the stripper was specified to release exactly the CO_2 captured. The closed solvent loop, including water and MEA make-up balances, was converged to a relative tear tolerance of 10^{-5}. At the scale of the industrial columns the RateSep residual reached a numerical floor near 2×10^{-5}; a relative tolerance of 10^{-4} was therefore used for the columns, corresponding to mass and energy balance closure better than 0.01%. Convergence of the industrial absorber required continuation (homotopy) initialisation and a top-stage temperature estimate below the lean solvent temperature.

Table 1. Design basis of the reference and hybrid plants.

Item	Value	Source
Flue gas per train (NGCC)	34,601.5 kmol h^{-1}, 99 °C, 1.0 bar	[12], 25% of stream 4
NGCC composition (mol%)	CO_2 4.08, H_2O 8.75, N_2 74.28, O_2 12.00, Ar 0.89	[12]
Coal flue gas, CO_2 (dry)	14.66 mol%	[12], Case B12B.90
Cement flue gas, CO_2 (dry)	20 mol% (range 14–35%)	[13]
CO_2 capture	90% overall	[12]
Solvent	30 wt% MEA (CO_2-free basis), lean loading 0.20	[2], this work
Absorber / stripper packing	FLEXIPAC 250Y, 20 m / 15 m	[14]
Stripper pressure, condenser	2.0 bar, 40 °C	[2], [20]
Lean/rich exchanger	ΔT_{min} = 10 K	this work
CO_2 product	15.3 MPa, 30 °C	[12]
Membrane material	Matrimid 5218, 35 °C	[11]
Membrane CO_2 recovery / amine capture	0.947 / 0.95	this work

2.4 Lean loading optimisation and amine performance map

The lean loading of the reference plant was varied between 0.15 and 0.25 mol CO_2 mol^{-1} MEA at constant 90% capture to locate the minimum SRD. An amine performance map was then generated by varying the dry CO_2 fraction at the amine inlet from 4.47% (NGCC) to 40% at constant CO_2 flow, reducing the N_2, O_2 and Ar flows in their original proportions. At each point the absorber diameter was re-sized to approximately 70% of flooding and the lean/rich exchanger was held at ΔT_{min} = 10 K; where the rich solvent began to flash inside the exchanger, the internal pinch was verified from the zone analysis and the cold-end approach was raised until the internal approach reached 10 K. These map points were computed open-loop, with the absorber feed specified at the lean loading returned by the stripper; this is equivalent at steady state to the closed loop and avoids recycle convergence at each point. Above 40% CO_2, SRD was held at its 40% value, a conservative choice given the plateau discussed in Section 3.3.

The SRD is defined as the reboiler duty per unit of captured CO_2,

$$SRD = Q_{reb} / \dot{m}_{CO2} \quad (1)$$

2.5 CO_2 compression

The CO_2 product was compressed from 2.0 bar to 15.3 MPa in five intercooled stages at equal pressure ratio, with an isentropic efficiency of 0.80, intercooling to 40 °C and after-cooling to 30 °C. Because the electrolyte property method is not intended for dense-phase CO_2, the compression work was cross-checked against an independent calculation using the Span–Wagner reference equation of state [21] implemented in CoolProp [22].

2.6 Membrane model

The membrane stage was described with the competitive dual-mode, partial-immobilisation model developed and calibrated in [11]. The sorbed concentration of gas i in the presence of gas j is

$$C_i = k_{D,i}\, p_i + C'_{H,i}\, b_i\, p_i / (1 + b_i\, p_i + b_j\, p_j) \tag{2}$$

and the steady flux through a membrane of thickness ℓ is

$$N_i = [D_{D,i}\,(C_{D,i,f} - C_{D,i,p}) + D_{H,i}\,(C_{H,i,f} - C_{H,i,p})] / \ell \tag{3}$$

where the subscripts f and p denote the feed and permeate faces. The effective mixed-gas permeability follows as $P_i = N_i\, \ell / (p_{i,f} - p_{i,p})$. The CO_2 behaviour is governed by the product $F{\cdot}K$, where $F = D_H/D_D$ is the mobility ratio and $K = C'_H b/k_D$. Sorption parameters were taken from Moore and Koros [23] (CO_2: k_D = 1.42 cm^3(STP) cm^{-3} bar^{-1}, C'_H = 25.5 cm^3(STP) cm^{-3}, b = 0.367 bar^{-1}; N_2: k_D = 0.118, C'_H = 3.94, b = 0.087), and the diffusivities were constrained to reproduce a pure-gas CO_2 permeability of 5.464 Barrer at 4 bar and an N_2 permeability of 0.19 Barrer, as in [11]. The primary value $F{\cdot}K$ = 0.191 and its interval 0.123 to 0.272 were calibrated in [11] against two independent datasets; the full interval was propagated here.

The module is a counter-current hollow-fibre permeator [24] discretised into 50 axial elements and solved by under-relaxed successive substitution. For each component the feed- and permeate-side molar flows obey

$$dF^f{}_i/dz = -a\, J_i, \quad dF^p{}_i/dz = -a\, J_i \tag{4}$$

with the permeate flowing opposite to the feed and J_i the local flux. Two design bases were compared. In design A, the membrane is sized with pure-gas permeabilities evaluated at 1 bar; in design B, the mixed-gas fluxes of Eqs. (2) and (3) are used throughout and represent the true behaviour of the material. The module feed is expressed through the dimensionless flow parameter

$$F_{in} = \varphi \cdot S\,[P_{CO2}\, y + P_{N2}(1 - y)]\,(p_f - p_p)\, a\, L \tag{5}$$

where S converts permeability to permeance and y is the feed CO_2 fraction. For each design basis, φ was solved by root finding so that the module achieves R_{mem} = 0.947, and the total area for a train follows by scaling the module to the full flue gas flow. Industrial asymmetric hollow fibres were represented by a selective skin of 0.1 μm, which scales area but leaves recovery and purity unchanged. O_2 and Ar were lumped with N_2 and the feed was taken as dehydrated, consistent with the binary model. Four driving-force configurations were evaluated, all at a pressure ratio of 10 except the 5/1 case: 1.1/0.11 bar (vacuum), 2.0/0.2 bar, 5/1 bar and 10/1

bar (compression). The model code was first used to reproduce the module-level results of [11]: for a 10/1 bar feed at a reference pressure of 1 bar, pure-gas design overestimated recovery by 2.53 percentage points and purity by 1.15 to 1.17 points, as reported.

2.7 Energy and cost model

Feed compressors, vacuum pumps and retentate expanders were modelled as intercooled ideal-gas machines with at most a pressure ratio of 3 per stage. The work of a machine with N stages is

$$W = N \dot{n} R T [k/(k - 1)] [r^{(k-1)/k} - 1] / \eta \quad (6)$$

with T = 313 K, k = 1.4 and efficiencies of 0.80 (compressor), 0.70 (vacuum pump) and 0.85 (expander, where the work is multiplied rather than divided by η). Reboiler steam was converted to an equivalent electrical penalty with a factor θ = 0.25 $MW_e\ MW_{th}^{-1}$. For a reboiler at 122.6 °C, the equivalent-work approach of Oyenekan and Rochelle [25] gives approximately 0.17 to 0.23; the adopted value therefore credits the hybrid generously for any steam saving. The equivalent energy of each configuration is

$$E = W_{comp} + W_{vac} - W_{exp} + \theta Q_{reb} \quad (7)$$

The cost comparison included only items that differ between configurations: membrane capital and replacement, machinery capital, the absorber, the blower and energy. The stripper, reboiler, CO_2 compression and the remainder of the MEA plant are identical in all cases because the captured CO_2 is the same, and cancel. The total annualised cost and the cost difference per tonne of CO_2 are

$$TAC = (CRF + f_{OM}) CAPEX + A c_m / \tau + E h c_{el} \quad (8)$$

$$\Delta c = (TAC_{hybrid} - TAC_{MEA}) / m_{CO2} \quad (9)$$

where A is the membrane area, c_m its installed cost, τ its lifetime, h the annual operating hours and c_{el} the electricity price. The absorber reference cost (USD 22 million for the 11.3 m reference column) is an assumption of this work; it was scaled with an exponent of 1.4 on diameter, equivalent to 0.7 on column volume at fixed height, consistent with the capacity exponents of 0.6 to 0.7 commonly used for process vessels [26]. Because this value is uncertain, it was varied from 0.5 to 3 times the base value in the sensitivity analysis (Section 3.8). Base and optimistic values are listed in Table 2. Two further simplifications favour the hybrid. First, the hybrid SRD was read from the amine map generated at 90% capture, whereas the hybrid requires the amine plant to capture 95% of the CO_2 it receives; because SRD increases with capture rate, the hybrid regeneration duty is underestimated. Second, θ = 0.25 exceeds the

equivalent-work estimate, which overvalues any steam saving. Both choices make the comparison conservative with respect to the conclusion.

Table 2. Economic and technical assumptions. Membrane cost assumptions follow [3], [5].

Parameter	Base	Optimistic	Sensitivity range
Membrane installed cost (USD m^{-2})	50	20	0–100
Membrane lifetime (y)	5	8	3–10
Machinery installed cost (USD kW^{-1})	1000	600	500–1500
Electricity price (USD MWh^{-1})	60	60	30–120
Absorber reference cost (MUSD, D = 11.3 m)	22	22	11–66
Steam-to-power factor θ	0.25	0.25	0.15–0.35
Capital recovery factor	0.0937	0.0937	0.06–0.12
Fixed O&M (fraction of CAPEX)	0.04	0.04	–
Operating hours (h y^{-1})	8000	8000	–
Compressor / vacuum / expander efficiency	0.80 / 0.70 / 0.85	same	0.70–0.88 / 0.60–0.80 / 0.75–0.90

2.8 Sensitivity analysis

Each parameter in Table 2 and a ±5% perturbation of the hybrid SRD were varied one at a time for the most favourable hybrid design of each source. In addition, all parameters were set simultaneously to the values most favourable to the hybrid (zero membrane cost, longest membrane life, cheapest and most efficient machinery, highest absorber cost, highest steam value and electricity price, lowest capital recovery factor and lowest hybrid SRD), and all four driving-force configurations were re-evaluated to identify the best case.

2.9 High-performance membrane bounding case

To test whether the conclusion is specific to Matrimid, the hybrid was re-evaluated with a membrane representative of commercial post-combustion membranes such as Polaris [3]: a CO_2 permeance of 1000 GPU and a CO_2/N_2 selectivity of 50, with constant permeances (solution-diffusion behaviour, no mixed-gas coupling). The same module model, recovery target, sources, pressure configurations and cost model were used, with the membrane cost at its base value, at zero, and with all parameters at their most hybrid-favourable values.

3. Results and discussion

3.1 Validation of the MEA model

Table 3 compares the rebuilt model with the AspenTech reference model and the Kaiserslautern measurements. The rebuilt model reproduces the reference model to within 0.1 percentage points of removal and 0.01 GJ t^{-1} of SRD, and the closed loop converges with consistent water

and MEA make-up. Relative to the pilot data, removal is under-predicted by 3.6 points and the rich loading by 0.02 mol mol^{-1}, while the SRD is over-predicted by 14%; the latter reflects the absence of heat losses in the model, which the pilot data exclude only approximately. These deviations are characteristic of rate-based MEA models applied to this pilot and represent the accuracy of the framework rather than of the rebuild.

Table 3. Validation against the Kaiserslautern pilot plant, case 1.

Quantity	This work	Reference model [14]	Pilot plant [20]
CO_2 removal (%)	72.5	72.6	76.1
Lean loading (mol mol^{-1})	0.253	0.254	0.262
Rich loading (mol mol^{-1})	0.365	0.365	0.387
SRD (GJ t^{-1})	5.73	5.72	5.01
Reboiler duty (kW)	7.05	7.05	6.47
Lean/rich exchanger duty (kW)	12.63	12.62	13.52
Make-up water (kg h^{-1})	2.28	2.22	1.95

3.2 Industrial reference plant

The NGCC reference train captures 55.9 t h^{-1} of CO_2 (90.0%, matching the NETL basis across four trains within 0.1%) with a solvent circulation of 965 t h^{-1}, lean and rich loadings of 0.200 and 0.481, a reboiler duty of 60.2 MW at 122.6 °C and an SRD of 3.88 GJ t^{-1}. The absorber requires a diameter of 11.3 m and the stripper 4.6 m. Cooling the treated gas to 40 °C recovers 37.5 t h^{-1} of water and reduces MEA losses from about 250 kg h^{-1} to 0.5 kg h^{-1}, leaving a make-up water demand of 0.66 t h^{-1}. The blower requires 1.72 MW. The SRD lies close to the 3.9 GJ t^{-1} reported by Abu-Zahra et al. for a comparable 30 wt% MEA base case [2].

Lean loadings of 0.15, 0.20 and 0.25 gave SRDs of 3.97, 3.88 and 3.98 GJ t^{-1} with circulation rates of 811, 965 and 1203 t h^{-1}. A parabola through these points places the minimum at 0.198, so the reference operates at its energy optimum. At low lean loading the additional stripping steam dominates, and the reboiler temperature rises to 123.8 °C; at high lean loading the larger circulation dominates through sensible heat. The minimum approach constraint in the lean/rich exchanger proved important: with only the hot-end approach fixed at 10 K, the cold end fell to 5 K and the SRD was 3.77 GJ t^{-1}, 0.11 GJ t^{-1} lower than on the consistent ΔT_{min} basis adopted here.

Compression to 15.3 MPa requires 4.97 MW per train (88.9 kWh t^{-1}). The Span–Wagner calculation gives 4.88 MW, within 2%, and confirms a dense-phase outlet density of 850 kg m^{-3}. NETL reports 4.48 MW per train; at an isentropic efficiency of 0.85 our calculation gives 4.60 MW, within 3%, indicating that the difference arises from machine efficiency.

3.3 Response of the MEA plant to feed enrichment

Fig. 2 and Table 4 summarise the amine performance map. Raising the dry CO_2 fraction at the absorber inlet from 4.5% to 40% reduces the SRD from 3.88 to 3.58 GJ t^{-1}, a reduction of only 7.7%. The decrease is concentrated below about 20%: between 30% and 40% the SRD changes by 0.01 GJ t^{-1}. The absorber diameter falls from 11.3 to 6.0 m, a much larger relative change that arises mainly from the reduced gas volume.

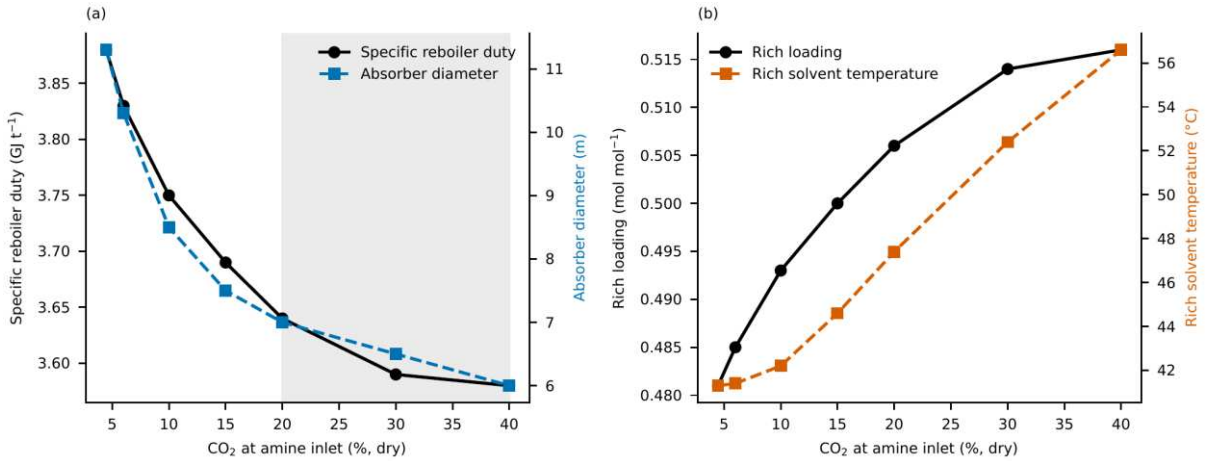


Fig. 2. Amine performance map at 90% capture and constant CO_2 flow, versus dry CO_2 fraction at the amine inlet. (a) Specific reboiler duty and absorber diameter (sized at approximately 70% of flooding); shading marks the 20–40% range, over which SRD varies by less than 0.06 GJ t^{-1}. (b) Rich loading and rich-solvent temperature at the absorber outlet.

Table 4. Amine performance map (lean loading 0.20, 90% capture, ΔT_{min} = 10 K).

CO_2 at inlet (%, dry)	SRD (GJ t^{-1})	Reboiler (MW)	Circulation (t h^{-1})	Rich loading	Absorber *D* (m)
4.47	3.88	60.2	965	0.481	11.3
6	3.83	59.5	949	0.485	10.3
10	3.75	58.3	923	0.493	8.5
15	3.69	57.3	900	0.500	7.5
20	3.64	56.6	882	0.506	7.0
30	3.59	55.7	861	0.514	6.5
40	3.58	55.6	854	0.516	6.0

Two mechanisms cap the benefit (Fig. 2b). First, the rich loading rises only from 0.481 to 0.516 mol mol^{-1}: 30 wt% MEA at 40 °C already approaches its practical loading ceiling at NGCC conditions, so the working capacity, and with it the solvent circulation and the sensible heat demand, change little. Second, the heat of absorption is released into a progressively smaller gas flow, so the rich solvent leaves the absorber hotter, from 41.3 °C at 4.5% to 56.6 °C at 40%. The lean/rich exchanger then pinches at its cold end, and at the highest loadings internally where CO_2 begins to flash from the rich solvent (near 96 to 100 °C on the cold side), which limits heat recovery and delivers the rich solvent to the stripper at a lower temperature. The

reboiler must supply the difference. The consequence for hybrid design is direct: enriching flue gas beyond roughly 20 to 30% CO_2 offers essentially no further reduction in regeneration energy.

3.4 Membrane stage performance

Fig. 3 shows the permeate composition delivered to the amine plant and the membrane area required per train when the stage is sized for $R_{mem} = 0.947$ with mixed-gas transport. Because high recovery forces a large stage cut, enrichment is modest: the permeate reaches 17.5 to 17.7% CO_2 for NGCC, 44 to 46% for coal and 54 to 56% for cement at a pressure ratio of 10, and only 12.4%, 35.6% and 45.4% at 5/1 bar, where the pressure ratio limits separation. At constant pressure ratio, the permeate composition is almost independent of absolute pressure, whereas the area decreases in proportion to the transmembrane pressure difference: for NGCC it falls from 27.7×10^6 m^2 per train under vacuum to 3.2×10^6 m^2 at 10/1 bar. These areas are large because Matrimid has a modest permeance (55 GPU at 0.1 µm) and the stage must process the full flue gas flow.

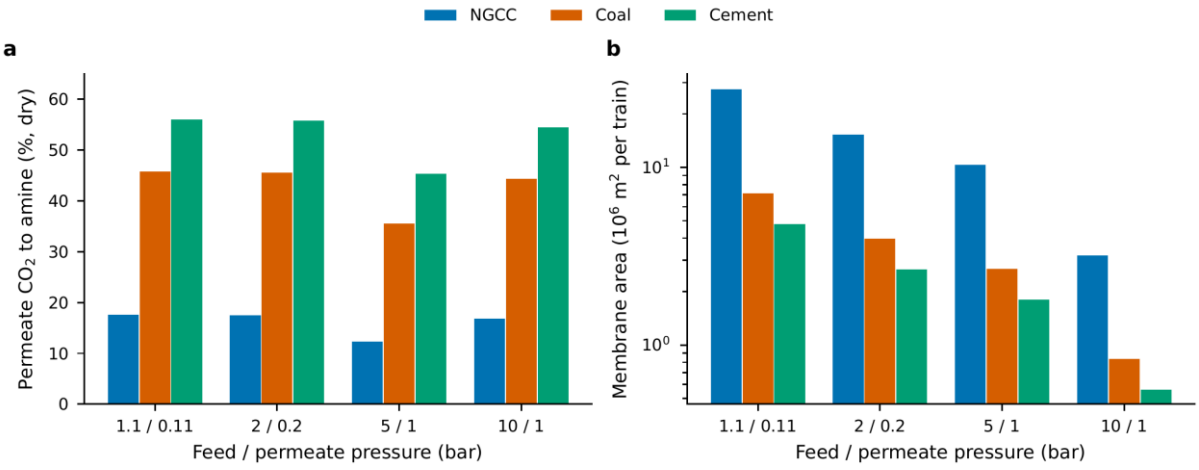


Fig. 3. Membrane stage sized for 94.7% CO_2 recovery with mixed-gas transport ($F{\cdot}K = 0.191$). (a) Dry CO_2 fraction in the permeate sent to the amine plant. (b) Membrane area per train (logarithmic scale), for four feed/permeate pressure combinations.

3.5 Consequences of pure-gas membrane design

Fig. 4 shows the error introduced when the membrane is sized with pure-gas permeabilities (design A) while the material behaves according to competitive mixed-gas transport (design B). Under vacuum operation the error is small and of either sign: the area deviates by −0.6 to +2.0% across the $F{\cdot}K$ interval and overall capture remains within 89.9 to 90.3%. At 2/0.2 bar the deviation remains within ±1.3%. Under feed compression the pure-gas design systematically undersizes the membrane, by 2.3 to 3.5% at 5/1 bar and by 4.0 to 6.5% at 10/1 bar, so that the plant built to the pure-gas design captures only 88.7 to 89.4% instead of 90%.

The trend is nearly identical for the three sources and widens with $F{\cdot}K$, as expected from the module-level analysis in [11].

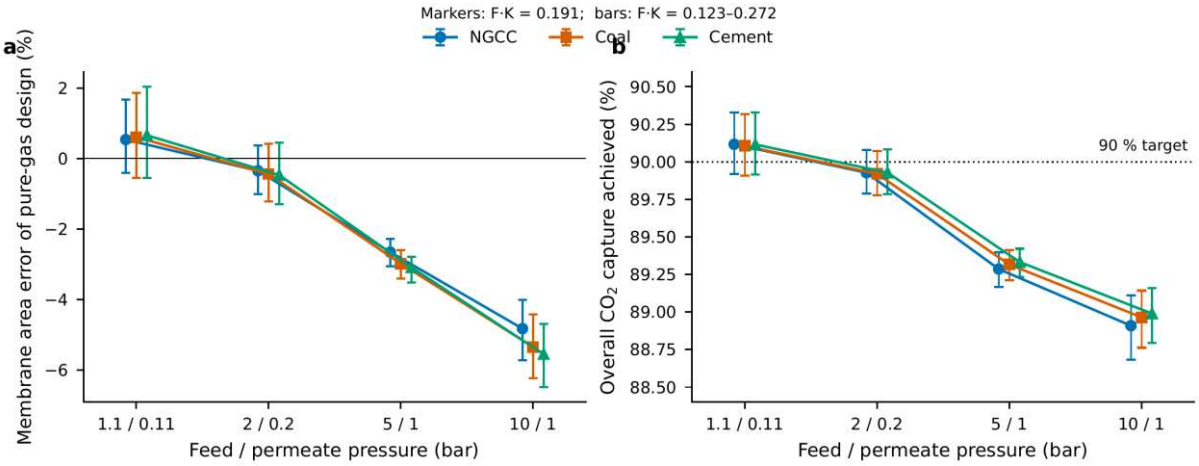


Fig. 4. Consequences of sizing the membrane with pure-gas permeabilities (measured at 1 bar) instead of mixed-gas transport. (a) Relative error in membrane area (negative values indicate undersizing). (b) Overall CO_2 capture achieved by the plant built to the pure-gas design. Markers correspond to $F{\cdot}K$ = 0.191; bars span $F{\cdot}K$ = 0.123 to 0.272.

The mechanism follows from Eq. (2). Near atmospheric feed pressure the partial pressures of both gases are low, the Langmuir sites are far from saturation and N_2 barely competes, so the mixed-gas CO_2 permeability approaches the pure-gas value at 1 bar. When the feed is compressed, the N_2 partial pressure of several bar occupies Langmuir sites that would otherwise sorb CO_2, lowering CO_2 permeability below the pure-gas reference; the pure-gas design then overestimates the flux and specifies too little area. The result holds across feed compositions from 4.5% to 20% CO_2, since it is driven mainly by the N_2 partial pressure. Economically the error is modest in the present context: the CO_2 left uncaptured by an undersized compression-driven stage is worth USD 0.04 to 0.66 million per train per year at USD 100 t^{-1}, small relative to the cost penalty of the hybrid itself (Section 3.7). Technically, however, it causes the plant to miss its design capture target by up to 1.3 percentage points, which matters for any membrane process operated under feed compression, including stand-alone membrane capture and partial-capture designs.

3.6 Energy comparison

Table 5 compares the equivalent energy of the MEA-only plant and the hybrid configurations. For every source and configuration, the hybrid requires more energy. The smallest penalties occur under vacuum operation (1.1/0.11 bar): +111% for NGCC, +48% for coal and +41% for cement. Feed compression to 10 bar increases the penalty to +280%, +99% and +77%. The reason is visible in the SRD column: even when the permeate reaches 46 to 56% CO_2, the SRD

decreases only from 3.69 or 3.64 GJ t^{-1} (coal and cement MEA-only) to 3.58 GJ t^{-1}, worth less than 0.4 MW of equivalent power per train, whereas vacuum pumping of a permeate representing 26% of the flue gas costs several megawatts. Under compression, the expander recovers about one third of the feed compression work but cannot close the gap.

Table 5. Equivalent energy per train for MEA-only and hybrid plants ($F{\cdot}K$ = 0.191; CO_2 compression excluded as common to all cases).

Source	Configuration (bar)	Permeate CO_2 (%)	SRD (GJ t^{-1})	*E* hybrid (MW_e)	*E* MEA-only (MW_e)
NGCC	1.1 / 0.11	17.7	3.66	35.5 (+111%)	16.8
NGCC	10 / 1	16.9	3.67	63.7 (+280%)	16.8
Coal	1.1 / 0.11	45.9	3.58	22.0 (+48%)	14.9
Coal	10 / 1	44.4	3.58	29.6 (+99%)	14.9
Cement	1.1 / 0.11	56.1	3.58	20.5 (+41%)	14.5
Cement	10 / 1	54.6	3.58	25.7 (+77%)	14.5

3.7 Cost comparison

Fig. 5 decomposes the annualised cost of the compared items for the cheapest hybrid design of each source. In the base case the MEA-only cost of these items is USD 19 to 25 t^{-1}, dominated by the steam equivalent, whereas the best hybrids cost USD 58 (cement), 75 (coal) and 221 t^{-1} (NGCC), all at 10/1 bar. Across all configurations the hybrid is more expensive by USD 39 to 187 t^{-1} for cement, 55 to 276 t^{-1} for coal and 196 to 1057 t^{-1} for NGCC. With optimistic assumptions (membrane at USD 20 m^{-2} with an eight-year life and machinery at USD 600 kW^{-1}) the penalties fall to USD 22 to 63, 30 to 91 and 102 to 341 t^{-1}, respectively, but remain positive in every case. The breakdown shows that the hybrid penalty is carried by the membrane and the machinery; the steam saving is barely perceptible, and the saving on the absorber, though real, is an order of magnitude smaller than the added items.

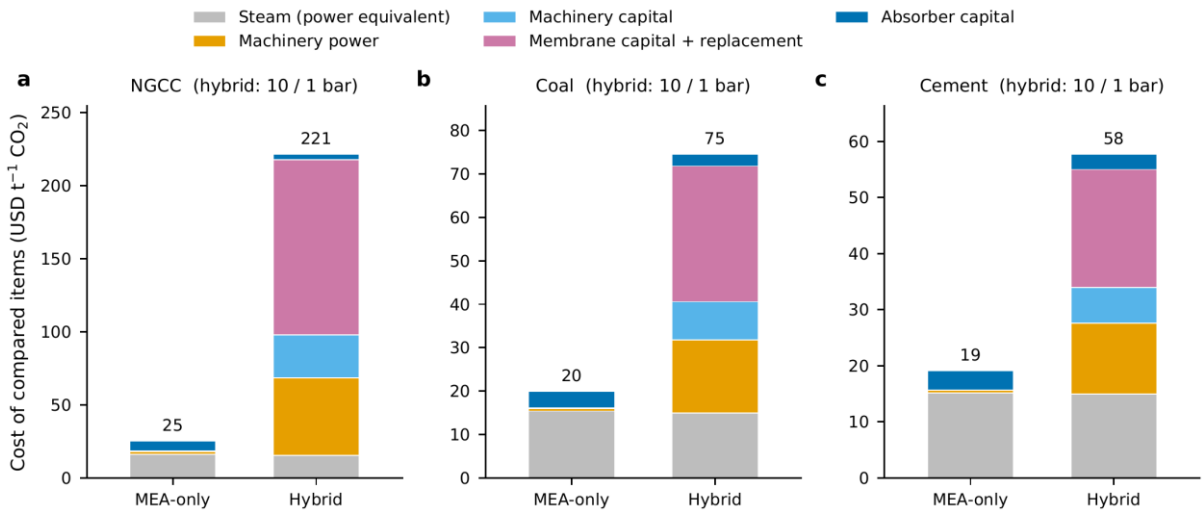


Fig. 5. Annualised cost of the items that differ between configurations, per tonne of CO_2 captured, for the MEA-only plant and the lowest-cost hybrid design of each source (base assumptions). (a) NGCC. (b) Coal. (c) Cement. Totals are shown above the bars.

3.8 Robustness of the economic conclusion

Fig. 6 shows the one-at-a-time sensitivity for cement, the source most favourable to the hybrid. From a base penalty of USD 38.6 t^{-1}, the membrane cost produces the largest swing (USD 18 to 60 t^{-1}), followed by the electricity price (33 to 51) and the membrane lifetime (32 to 47). Machinery cost, capital recovery factor and compressor efficiency have moderate effects, while the steam-to-power factor, absorber cost, vacuum and expander efficiencies and a ±5% change in the hybrid SRD alter the result by at most about USD 2 t^{-1}. No single parameter brings the penalty to zero. The same ranking holds for coal (base USD 54.7 t^{-1}) and NGCC (USD 196 t^{-1}).

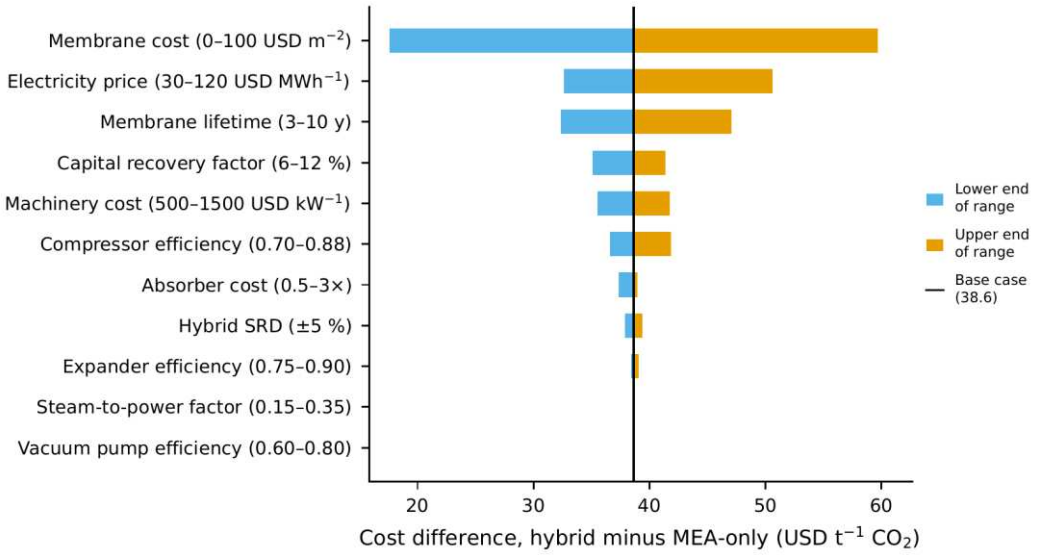


Fig. 6. One-at-a-time sensitivity of the cost difference between the lowest-cost hybrid and the MEA-only plant for cement flue gas. Bars span the result at the lower and upper ends of each parameter range.

When all parameters were set simultaneously to their most hybrid-favourable values, including a membrane of zero cost, the best configuration shifted to vacuum operation and the penalty fell to USD 26.6 t^{-1} for NGCC, 9.0 t^{-1} for coal and 7.9 t^{-1} for cement, still positive in every case. Even without any membrane cost, the power and capital of the vacuum pumps or compressors exceed what the amine plant can save. For the Matrimid stage, the conclusion is therefore not contingent on membrane price within the explored range; it follows from the plateau in MEA regeneration energy combined with the cost of generating the membrane driving force. This is consistent with the observation from membrane pilot programmes that compression equipment, rather than membrane area, is the main economic barrier [3], [5], and it implies that pre-concentration would require an amine plant whose energy responds far more strongly to CO_2 partial pressure than 30 wt% MEA does.

3.9 High-performance membrane

Table 6. Hybrid cost penalty with a high-performance membrane (1000 GPU, CO_2/N_2 selectivity 50). The free-membrane and all-favourable values are the minima over the four pressure configurations.

Source	Best configuration (bar)	Permeate CO_2 (%)	Area (10^6 m^2)	Δ*c* base (USD t^{-1})	Δ*c* free membrane / all favourable
NGCC	2 / 0.2	20.0	1.24	79.9	20.0 / 21.2
Coal	2 / 0.2	50.6	0.31	23.3	8.1 / 7.6
Cement	2 / 0.2	61.1	0.20	17.2	7.0 / 6.9

Table 6 summarises the bounding case. Compared with Matrimid, the high-performance membrane reduces the area by more than an order of magnitude (0.2 to 2.2 × 10^6 m^2 per train under vacuum) and raises the permeate to 20% (NGCC), 51% (coal) and 61% (cement) CO_2. The cost penalty falls from USD 39 to 17 t^{-1} for cement and from USD 55 to 23 t^{-1} for coal at base assumptions, but remains positive in every configuration and for every source. With a free membrane the minimum penalties are USD 20.0, 8.1 and 7.0 t^{-1}, and with all parameters at their most favourable values USD 21.2, 7.6 and 6.9 t^{-1}. For NGCC the all-favourable value slightly exceeds the free-membrane value because the highest electricity price, favourable in the steam-dominated Matrimid case, penalises the machinery-dominated high-performance case. Even at a CO_2/N_2 selectivity of 50, recovering 94.7% of the CO_2 requires a stage cut of 21 to 31%, so a large permeate flow must still be vacuum-pumped or a large feed flow compressed, while the amine plant gains little from the higher enrichment because of the SRD plateau. Membrane performance therefore narrows the gap substantially but does not reverse the conclusion for single-stage pre-concentration ahead of 30 wt% MEA. The mixed-gas design error of Section 3.5 does not arise in this idealised case, which assumes constant permeances

without Langmuir-site competition; it is specific to glassy polymers described by dual-mode sorption.

3.10 Comparison with earlier hybrid studies, implications and limitations

The present conclusions are consistent with the finding of Cormos et al. that chemical absorption alone retains a higher net efficiency than solvent–membrane hybrids for supercritical coal plants [7], and with the MTR/UT Austin conclusion that a membrane–piperazine hybrid did not materially reduce the cost of capture relative to the solvent alone [6], even though that work used a more advanced solvent, membrane contactors and parallel arrangements rather than single-stage pre-concentration. By contrast, the advantage reported for membrane–liquefaction hybrids [8] relies on a downstream process whose energy decreases strongly with permeate concentration. The present results therefore do not argue against hybrid capture in general; they show that the specific combination of single-stage pre-concentration and 30 wt% MEA is unfavourable, and they identify the SRD plateau as the reason.

Three practical implications follow. First, for 30 wt% MEA the regeneration energy is largely insensitive to feed CO_2 concentration above about 20%, so flue gas enrichment cannot be justified on regeneration energy, and only marginally on absorber size. Second, for the sources examined, a Matrimid pre-concentration stage increases both energy and cost under every assumption tested, independently of membrane cost, and a membrane with 1000 GPU and a selectivity of 50 narrows but does not close the gap. Third, where glassy-polymer membranes are used in post-combustion service, vacuum-driven stages are preferable not only for energy but also because they are insensitive to the pure-gas design error; compression-driven stages should be designed with mixed-gas transport data.

The analysis has limitations. The membrane model is binary and isothermal; O_2 was lumped with N_2, water was assumed removed upstream, and plasticisation and physical ageing were not represented. Only single-stage membranes in series with the amine plant were considered, and the high-performance case used idealised constant permeances; parallel or retentate-polishing arrangements, partial capture and solvents with stronger dependence on CO_2 partial pressure (for example, piperazine blends or advanced amines) may behave differently. The amine map was generated at 90% capture and applied to the 95% capture required in the hybrid, which underestimates the hybrid SRD. The map extends to 40% CO_2 and was extrapolated as constant beyond it, and absorber capital was represented by a scaling law rather than detailed equipment costing. CO_2 compression and the stripper, being common to all cases, were

excluded from the comparison, so absolute capture costs are not reported. None of these simplifications is expected to change the direction of the conclusions, given the margins observed in the sensitivity analysis.

4. Conclusions

A rate-based MEA model, validated against pilot-plant data and scaled to the NETL NGCC baseline, was combined with a competitive dual-mode hollow-fibre membrane model to evaluate membrane pre-concentration ahead of MEA absorption for NGCC, coal and cement flue gases. The main findings are:

(i) The optimised NGCC reference plant requires an SRD of 3.88 GJ t^{-1} at a lean loading of 0.20, with 4.97 MW per train for CO_2 compression, in agreement with an independent Span–Wagner calculation and the NETL baseline.

(ii) The SRD of 30 wt% MEA falls by only 7.7%, from 3.88 to 3.58 GJ t^{-1}, as the inlet CO_2 fraction rises from 4.5% to 40%, and is nearly constant above 20 to 30%, because rich loading approaches its ceiling and the hotter rich solvent pinches the lean/rich exchanger.

(iii) A Matrimid stage sized to pass 94.7% of the CO_2 enriches the feed only to 17.7% (NGCC), 46% (coal) and 56% (cement), and the resulting hybrids consume 41 to 280% more equivalent energy and cost USD 22 to 1057 t^{-1} more than MEA alone.

(iv) The hybrid remains more expensive under all assumptions tested, including zero membrane cost, with a minimum penalty of USD 7.9 t^{-1} for cement; membrane cost, electricity price and membrane lifetime dominate the sensitivity. A high-performance membrane (1000 GPU, selectivity 50) lowers the penalty to USD 7 to 80 t^{-1} but does not remove it at base assumptions, and to no less than USD 7 t^{-1} with a free membrane.

(v) Sizing the membrane with pure-gas permeabilities undersizes compression-driven stages by up to 6.5% and reduces overall capture to as little as 88.7%, while vacuum-driven stages are unaffected, extending the module-level findings of [11] to the plant scale.

Single-stage membrane pre-concentration is therefore not recommended ahead of 30 wt% MEA for these sources. Future work should test solvents whose regeneration energy depends more strongly on CO_2 partial pressure, alternative membrane–amine arrangements and partial-capture targets, and should incorporate mixed-gas transport in any compression-driven membrane design.

Data availability

The Aspen Plus models (pilot validation and industrial reference plant), the Python script reproducing all membrane, energy, cost and sensitivity calculations and Figs. 2 to 6, and the generated results are openly available at https://doi.org/10.5281/zenodo.23263315.

CRediT authorship contribution statement

Miracle Victory Ajoku: Conceptualization, Methodology, Software, Validation, Formal analysis, Investigation, Data curation, Visualization, Writing – original draft, Writing – review & editing.

Funding

This research did not receive any specific grant from funding agencies in the public, commercial or not-for-profit sectors.

Declaration of competing interest

The author declares no known competing financial interests or personal relationships that could have appeared to influence the work reported in this paper.

Declaration of generative AI and AI-assisted technologies in the writing process

The study design, process modelling, simulations, validation and interpretation of results were carried out by the author. During manuscript preparation, the author used Claude (Anthropic) as a support tool for language editing, for help with writing and debugging parts of the analysis and plotting code, and for checking literature sources. All AI-assisted output was reviewed, tested and revised by the author, and all reported results were verified against the original Aspen Plus simulations and model outputs. The author takes full responsibility for the content of this publication.

References

[1] G. T. Rochelle, "Amine scrubbing for CO_2 capture," *Science*, vol. 325, no. 5948, pp. 1652–1654, 2009.

[2] M. R. M. Abu-Zahra, L. H. J. Schneiders, J. P. M. Niederer, P. H. M. Feron, and G. F. Versteeg, "CO_2 capture from power plants: Part I. A parametric study of the technical performance based on monoethanolamine," *Int. J. Greenh. Gas Control*, vol. 1, no. 1, pp. 37–46, 2007.

[3] T. C. Merkel, H. Lin, X. Wei, and R. Baker, "Power plant post-combustion carbon dioxide capture: An opportunity for membranes," *J. Membr. Sci.*, vol. 359, no. 1–2, pp. 126–139, 2010.

[4] L. M. Robeson, "The upper bound revisited," *J. Membr. Sci.*, vol. 320, no. 1–2, pp. 390–400, 2008.

[5] R. W. Baker, T. C. Merkel, and B. C. Freeman, "Large pilot testing of the MTR membrane post-combustion CO_2 capture process (DE-FE0031587)," presented at the NETL CO_2 Capture Technology Meeting, Pittsburgh, PA, USA, Aug. 2018.

[6] B. Freeman, J. Kniep, R. Baker, T. Merkel, P. Hao, G. Rochelle, E. Chen, Y. Zhang, J. Ding, and B. Sherman, "Bench scale development of a hybrid membrane-absorption CO_2 capture process (DE-FE0013118)," presented at the NETL CO_2 Capture Technology Project Review Meeting, Pittsburgh, PA, USA, Aug. 2018.

[7] C.-C. Cormos, L. Petrescu, A.-M. Cormos, and C. Dinca, "Assessment of hybrid solvent–membrane configurations for post-combustion CO_2 capture for super-critical power plants," *Energies*, vol. 14, no. 16, art. 5017, 2021.

[8] R. Anantharaman, D. Berstad, and S. Roussanaly, "Techno-economic performance of a hybrid membrane–liquefaction process for post-combustion CO_2 capture," *Energy Procedia*, vol. 61, pp. 1244–1247, 2014.

[9] D. R. Paul and W. J. Koros, "Effect of partially immobilizing sorption on permeability and the diffusion time lag," *J. Polym. Sci. Polym. Phys. Ed.*, vol. 14, no. 4, pp. 675–685, 1976.

[10] W. J. Koros, R. T. Chern, V. Stannett, and H. B. Hopfenberg, "A model for permeation of mixed gases and vapors in glassy polymers," *J. Polym. Sci. Polym. Phys. Ed.*, vol. 19, no. 10, pp. 1513–1530, 1981.

[11] M. V. Ajoku, M. Sola-Ojo, and G. C. Duru, "Can pure-gas permeability data design a mixed-gas module? A correctability map for dual-mode CO_2/N_2 transport in Matrimid 5218 hollow fibres," Research Square (preprint), Nov. 2026, doi: 10.21203/rs.3.rs-11646086/v1.

[12] T. Schmitt *et al.*, "Cost and performance baseline for fossil energy plants, Volume 1: Bituminous coal and natural gas to electricity," National Energy Technology Laboratory, Pittsburgh, PA, USA, Rev. 4a, Oct. 2022.

[13] R. Anantharaman et al., "CEMCAP framework for comparative techno-economic analysis of CO_2 capture from cement plants," CEMCAP Deliverable D3.2, Rev. 2, SINTEF Energy Research, Trondheim, Norway, 2018, doi: 10.5281/zenodo.1257112.

[14] Aspen Technology, Inc., "Rate-based model of the CO_2 capture process by MEA using Aspen Plus," Bedford, MA, USA, 2014.

[15] Y. Zhang, H. Que, and C.-C. Chen, "Thermodynamic modeling for CO_2 absorption in aqueous MEA solution with electrolyte NRTL model," *Fluid Phase Equilib.*, vol. 311, pp. 67–75, 2011.

[16] H. Hikita, S. Asai, H. Ishikawa, and M. Honda, "The kinetics of reactions of carbon dioxide with monoethanolamine, diethanolamine and triethanolamine by a rapid mixing method," *Chem. Eng. J.*, vol. 13, no. 1, pp. 7–12, 1977.

[17] B. R. W. Pinsent, L. Pearson, and F. J. W. Roughton, "The kinetics of combination of carbon dioxide with hydroxide ions," *Trans. Faraday Soc.*, vol. 52, pp. 1512–1520, 1956.

[18] J. L. Bravo, J. A. Rocha, and J. R. Fair, "Mass transfer in gauze packings," *Hydrocarbon Process.*, vol. 64, no. 1, pp. 91–95, 1985.

[19] J. Stichlmair, J. L. Bravo, and J. R. Fair, "General model for prediction of pressure drop and capacity of countercurrent gas/liquid packed columns," *Gas Sep. Purif.*, vol. 3, no. 1, pp. 19–28, 1989.

[20] R. Notz, H. P. Mangalapally, and H. Hasse, "Post combustion CO_2 capture by reactive absorption: Pilot plant description and results of systematic studies with MEA," *Int. J. Greenh. Gas Control*, vol. 6, pp. 84–112, 2012.

[21] R. Span and W. Wagner, "A new equation of state for carbon dioxide covering the fluid region from the triple-point temperature to 1100 K at pressures up to 800 MPa," *J. Phys. Chem. Ref. Data*, vol. 25, no. 6, pp. 1509–1596, 1996.

[22] I. H. Bell, J. Wronski, S. Quoilin, and V. Lemort, "Pure and pseudo-pure fluid thermophysical property evaluation and the open-source thermophysical property library CoolProp," *Ind. Eng. Chem. Res.*, vol. 53, no. 6, pp. 2498–2508, 2014.

[23] T. T. Moore and W. J. Koros, "Gas sorption in polymers, molecular sieves, and mixed matrix membranes," *J. Appl. Polym. Sci.*, vol. 104, no. 6, pp. 4053–4059, 2007.

[24] M. J. Thundyil and W. J. Koros, "Mathematical modeling of gas separation permeators: For radial crossflow, countercurrent, and cocurrent hollow fiber membrane modules," *J. Membr. Sci.*, vol. 125, no. 2, pp. 275–291, 1997.

[25] B. A. Oyenekan and G. T. Rochelle, "Alternative stripper configurations for CO_2 capture by aqueous amines," *AIChE J.*, vol. 53, no. 12, pp. 3144–3154, 2007.

[26] R. Turton, J. A. Shaeiwitz, D. Bhattacharyya, and W. B. Whiting, *Analysis, Synthesis, and Design of Chemical Processes*, 5th ed. Boston, MA, USA: Prentice Hall, 2018.